Highly efficient sorption and luminescence sensing of oxoanionic species by 8-connected alkyl-amino functionalized Zr^{4+} MOFs†

Anastasia D. Pournara,[a] Dimitrios A. Evangelou,[a] Christina Roukounaki,[c] Evangelos K. Andreou,[b] Gerasimos S. Armatas, [iD][b] Theodore Lazarides [iD][c] and Manolis J. Manos [iD] *[a,d]

In the present study we provide the sorption properties of four 8-connected Zr^{4+} MOFs with the general formula $H_{16}[Zr_6O_{16}(RNH-BDC)_4]\cdot$solvent ($RNH-BDC^{2-}$ = 2-alkyl-amine-terephthalate; R = ethyl-, **ET-MOF**; R = propyl-, **PROP-MOF**; R = isobutyl-, **SBUT-MOF**; R = *n*-butyl, **BUT-MOF**) towards toxic Cr(VI) and radionuclide-related ReO_4^- oxoanions. These MOFs represent superior sorbents for the removal of oxoanionic species, in terms of kinetics, sorption isotherms, selectivity and regeneration/reusability. The excellent sorption capability of the MOFs is due to a combination of surface and intra-framework sorption phenomena. The latter process proceeds *via* replacement of terminal water/hydroxyl ligands from the Zr_6 clusters and subsequent binding of oxoanions to the Zr^{4+} centers, a fact that was proved *via* Rietveld PXRD analysis for the anion-loaded **BUT-MOF**. Importantly, **BUT-MOF** demonstrated an exceptional sorption capacity for $Cr_2O_7^{2-}$ (505 mg g^{-1}) and was further utilized in a sorption column in the form of MOF/calcium alginate beads, displaying remarkable removal efficiency towards industrial (chrome-plating) wastewater. Furthermore, the luminescence Cr(VI) sensing properties of **BUT-MOF** were explored in detail, presenting high sensitivity (detection limits as low as 9 ppb) and selectivity for these species against various competitive anions.

Introduction

Water represents the largest natural resource and the source of life in every sense of the word, as it is the basis of the existence of most living organisms. However, the widespread growth of modern industry results in the extensive pollution of aquatic environments, which in turn poses a threat for humans and other living species. A certain number of in-organic pollutants, present in the form of oxoanions, are recorded as priority pollutants in the lists of the Environment Protection Agency (EPA) and the World Health Organization

[a]*Department of Chemistry, University of Ioannina, GR-45110 Ioannina, Greece. E-mail: emanos@uoi.gr*
[b]*Department of Materials Science and Technology, University of Crete, GR-71003 Heraklion, Greece*
[c]*Laboratory of Inorganic Chemistry, Department of Chemistry, Aristotle University of Thessaloniki, 54124 Thessaloniki, Greece*
[d]*Institute of Materials Science and Computing, University Research Center of Ioannina, GR-45110 Ioannina, Greece*

†Electronic supplementary information (ESI) available: Experimental procedures, details of Rietveld refinement, characterization and fluorescence titration data. CCDC 2204055–2204057. For ESI and crystallographic data in CIF or other electronic format see DOI: https://doi.org/10.1039/d2dt02848d

(WHO).[1,2] Compared to the cationic forms, which can be easily removed by several methods, including sorption or precipitation, the oxoanionic forms display higher solubility and environmental mobility, and can be transferred freely in the environment. A representative example of oxoanionic species is hexavalent chromium Cr(VI) which exists in the form of dichromate ($Cr_2O_7^{2-}$), hydrogen chromate ($HCrO_4^-$), or chromate (CrO_4^{2-}) depending on the pH values of the effluents. Hexavalent chromium is released in the environment through various industrial activities (electroplating, leather tanning *etc*.) and is highly toxic, with well-known carcinogenic and mutagenic properties.[3,4] TcO_4^- is also classified as an emergent oxoanionic contaminant since it is radioactive with long half-life ($t_{1/2}$ = 2.13 × 10^5 years) and high environmental mobility.[5]

Over the past decades, a variety of methods have dealt with the problem of the removal of these highly toxic oxoanions from aqueous media, including sorption, biological treatments, chemical oxidation/reduction, membrane filtration, and so on.[6–10] However, the greater part of these technologies suffers from disadvantages and the development of novel techniques and materials has been the subject of intensive study. Among the conventional techniques, the eco-friendly, simply

designed, low-cost, and highly efficient sorption, seems to be the most promising one.

Metal–organic frameworks (MOFs), an important class of porous materials, which are built from organic linkers and metal ions through coordination bonds, are considered as par excellence innovative materials for the sorption of contaminants from aqueous solutions and wastewater.[11–14] MOFs combine significantly larger surface areas than conventional sorbent materials and structural features, such as appropriate functional groups and ion-binding sites, and not surprisingly they are considered as the next generation sorbents.

Besides sorption, which leads the research on the environmental applications of MOFs, the detection–determination of contaminants is equally important.[15–17] MOFs with efficient fluorescence and capability to sorb ionic species are very promising materials for luminescence sensing applications. To date, relatively few examples of MOFs can combine both sorption and luminescence detection operations.[18]

Recently, we reported four new microporous Zr^{4+} MOFs with the general formula $H_{16}[Zr_6O_{16}(RNH-BDC)_4]\cdot$solvent ($RNH-BDC^{2-}$ = 2-alkyl-amine-terephthalate; R = ethyl-, **ET-MOF**; R = propyl-, **PROP-MOF**; R = isobutyl-, **SBUT-MOF**; R = *n*-butyl, **BUT-MOF**) (Fig. 1). These MOFs exhibited an 8-connected framework and displayed relatively large BET surface areas up to 832 m^2 g^{-1}.[19] These materials have shown excellent Se(IV/VI) and SeCN$^-$ sorption properties, with fast and selective capture of these anionic species under a variety of conditions. The highly efficient sorption properties of these materials arise from a combination of external surface and intra-framework sorption processes, with the latter been facilitated by the presence of labile-terminal OH$^-$/H$_2$O ligands easily replaced by the Se anionic species.[19]

Herein, we extend our studies towards the sorption of the toxic Cr(IV) and perrhenate (ReO$_4^-$) species, with the latter be considered as a model for the radioactive TcO$_4^-$ anion. The

alkyl-amino functionalized MOFs exhibit some of the highest reported sorption capacities for Cr(VI) (up to 505 mg Cr$_2$O$_7^{2-}$ per g, 187 mg CrO$_4^{2-}$ per g) and particularly high selectivity *vs.* common competitive anions. Furthermore, we fabricated a sorption column with **BUT-MOF/calcium alginate** beads as stationary phase, which displayed efficient performance for the sorption of Cr(VI) from industrial waste samples, along with noticeable recyclability. In addition, the alkyl-amino functionalized MOFs showed highly efficient sorption properties towards ReO$_4^-$, revealing exceptional sorption capacities (up to 960 mg ReO$_4^-$ per g) and excellent performance over a broad pH range, including concentrated HNO$_3$ solutions simulating acidic nuclear waste.[20] Besides the excellent sorption properties, **BUT-MOF** displays selective luminescence sensing properties towards Cr(VI) showing particularly low detection limits, well-below the maximum permissible level of Cr(VI) in drinking water. Overall, the present work emphasizes on the multifunctionality of microporous Zr^{4+} MOFs with low net-connectivity, showing capability for rapid and efficient capture of multiple anionic pollutants as well as selective luminescence-based detection of such species in aqueous media.

Results and discussion

Batch sorption studies

Our previous reported study revealed that alkyl-amino functionalized MOFs and especially **BUT-MOF** are very efficient sorbents for the decontamination of wastewater from Se species (including highly toxic SeCN$^-$ anions).[19] At the current study, we examine the ability of these MOFs to uptake several hazardous oxoanions, including Cr$_2$O$_7^{2-}$, CrO$_4^{2-}$ and ReO$_4^-$. The removal of Cr(VI) oxoanions from aqueous resources is crucial due to their considerable toxicity, whereas the capture of ReO$_4^-$ is of great interest given that it can be utilized as a model for TcO$_4^-$ sorption investigations.[3–5] In the following we present detailed batch Cr$_2$O$_7^{2-}$, CrO$_4^{2-}$ and ReO$_4^-$ sorption studies as well as column Cr$_2$O$_7^{2-}$ sorption data for **BUT-MOF**. Prior the sorption investigations, the MOF was activated *via* treatment with a HCl acid solution (ESI†).

Kinetic studies. The kinetic behaviour of **BUT-MOF** towards Cr$_2$O$_7^{2-}$, CrO$_4^{2-}$ and ReO$_4^-$ is depicted in Fig. 2 for time intervals from 1 to 10 minutes. **BUT-MOF** revealed rapid sorption
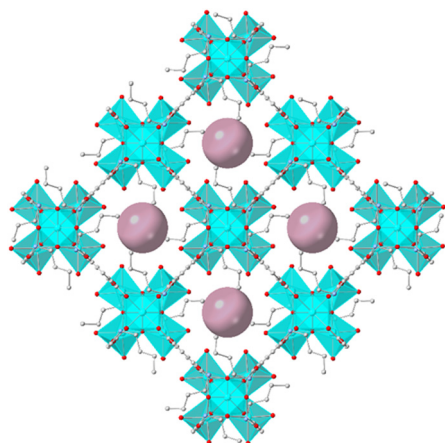
Fig. 1 Representation of the framework structure of **BUT-MOF** (C, gray; O, red; N, blue; and Zr turquoise). The H atoms and the solvent molecules in the structural representation of **BUT-MOF** were omitted for clarity. The large plum balls indicate the pores in the structure of **BUT-MOF**.
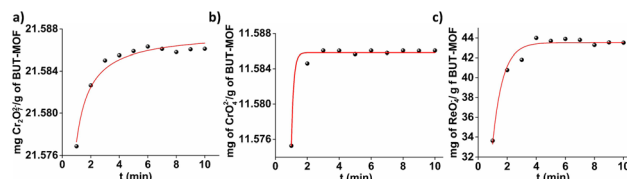
Fig. 2 Fitting of the kinetics data with the Ho-McKay's second order equation for the sorption of (a) Cr$_2$O$_7^{2-}$ (initial Cr$_2$O$_7^{2-}$ concentration = 21.6 ppm, pH ~ 3) and the Lagergren's pseudo-first-order equation for the sorption of (b) CrO$_4^{2-}$ (initial CrO$_4^{2-}$ concentration = 11.6 ppm, pH ~ 7), and (c) ReO$_4^-$ (initial ReO$_4^-$ concentration = 50 ppm, pH ~ 7) by **BUT-MOF**.

kinetics, with equilibrium reached within the first 3 minutes (Fig. 2a and b). Interestingly, **BUT-MOF** removed >99.9% of the initial Cr(VI) (C_i = 0.1 mM) in the first minute of contact with the solution of either $Cr_2O_7^{2-}$ or CrO_4^{2-}. A further increase in contact time had a negligible effect on the removal percentages. Both Lagergren's first order and Ho-McKay's second order kinetics models were used for the fitting of the kinetic data. The $Cr_2O_7^{2-}$ sorption of **BUT-MOF** can be described better with the Ho-McKay's second order equation, while the fitting of kinetics data towards CrO_4^{2-} anions was better achieved with Lagergren's first order equation (Table S1†).

We have also conducted time dependent sorption experiments of **BUT-MOF** towards ReO_4^- anions. In Fig. 2c is presented the variation of sorbed ReO_4^- on **BUT-MOF** as a function of reaction time, with the initial ReO_4^- concentration being 50 ppm. The kinetic investigations indicated that the capture of ReO_4^- by **BUT-MOF** was particularly fast and comparable to the uptake of chromium(VI) anions. The equilibrium was achieved at the 4th min of contact. Lagergren's first order equation was the best model for fitting the ReO_4^- kinetic data (Table S1†).

Sorption isotherm studies. The study of the sorption equilibrium isotherm is critical to evaluate the maximum sorption capacity of the sorbate for the given sorbent as well as to better understand the sorbate–sorbent interactions. Various isotherm models like Langmuir, Freundlich, and Langmuir–Freundlich, have been used to describe the equilibrium characteristics of sorption. Fig. 3 displays the sorption amount of Cr(VI) toxic species ($Cr_2O_7^{2-}$ and CrO_4^{2-}) as well as ReO_4^- ions on the **BUT-MOF** at different equilibrium concentrations. The Cr(VI) sorption isotherms of the **BUT-MOF** consist of two components. These results came with no surprise, since similar sorptive behaviour has been reported by our group previously for the Se(VI) and SeCN$^-$ sorption isotherms.[19] In general, this type of "two-steps isotherm" can be attributed to involvement of both surface binding and pore filling processes.[19,21] The maximum $Cr_2O_7^{2-}$ sorption capacity of **BUT-MOF** was found 505 mg $Cr_2O_7^{2-}$ per g, with 187 mg captured at the surface and 317 mg trapped in the framework. The latter value corresponds to 3.5 equivalents of dichromate per formula of the **BUT-MOF**. Furthermore, the sorption isotherms at pH ∼ 7, where Cr(VI) exists mainly in the form of CrO_4^{2-}, revealed that **BUT-MOF** was able to remove 153 mg of CrO_4^{2-} per g, which correspond to 65 mg CrO_4^{2-} per g trapped on the surface and 88 mg CrO_4^{2-} per g into the framework. The latter value is consistent with the insertion of 1.80 equivalents of chromate per formula unit of the MOF. The Cr(VI) sorption isotherm data at the first step can be fitted very well with the Langmuir model, whereas the Langmuir–Freundlich model can be applied for the fitting of the data at the second step (Fig. 3a and b). Besides its excellent performance towards Cr(VI) species, **BUT-MOF** was proved to be a first-rate sorbent for ReO_4^- ions. ReO_4^- sorption isotherm is also conformed to the two-step profile, fitted with Langmuir (first step) and Langmuir–Freundlich model (second step) (Fig. 3). **BUT-MOF** demonstrated outstanding sorption capacity, as high as 868 mg of ReO_4^- per g, with 354
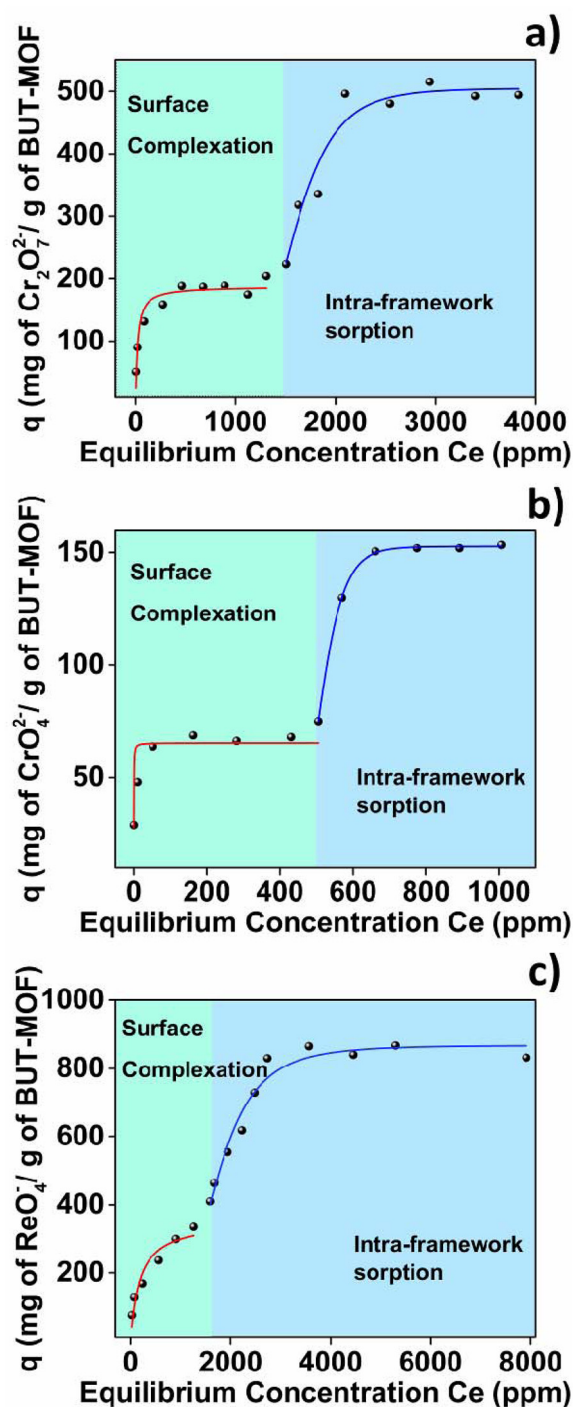

Fig. 3 (a) $Cr_2O_7^{2-}$, (b) CrO_4^{2-} and (c) ReO_4^- isotherm sorption data for **BUT-MOF** fitting with the various models. Red: Langmuir model; blue: Langmuir–Freundlich model.

and 514 mg ReO_4^- captured at the surface and in the framework, respectively. The latter value represents 4.8 equivalents of ReO_4^- per formula of **BUT-MOF**. The fitting parameters are summarized in Tables S2–S4.†

The excellent performance of **BUT-MOF** in ReO_4^- uptake impelled us further to investigate the sorption isotherms

under acidic and basic conditions. Interestingly, sorption isotherms conducted in HNO_3 solutions (1 M) revealed that **BUT-MOF** retains its excellent efficiency to remove ReO_4^- even under such extreme acidic conditions, achieving maximum sorption capacity as high as 776 mg g^{-1}, which is relatively close to that obtained at neutral solutions (Fig. S1; Table S5†). Should be pointed out here that HNO_3 solutions simulate acidic nuclear waste and subsequently **BUT-MOF** could be an attractive superior sorbent for nuclear waste remediation processes.[20] Isotherm study conducted in pH ∼ 9 revealed a decrease in the removal of ReO_4^- by **BUT-MOF** with maximum sorption capacity at 504 mg g^{-1} (Fig. S2; Table S5†). The reduced ReO_4^- sorption capacity of **BUT-MOF** in the alkaline environment can be explained by the fact that under such conditions the amine groups of the MOF may not be protonated and the surface sorption is less effective. Thus, there is a decrease in the surface sorption capability of **BUT-MOF**, leading to a smaller ReO_4^- sorption capacity under alkaline conditions. The sorption capacity of the other MOFs (**ET-**, **PROP-**, and **SBUT-MOF**) towards Cr(VI) anions was also investigated in detail (Fig. S3–S5†).

The Cr(VI) sorption isotherms of these MOFs consist of two components, with maximum sorption capacities in the range of 217–451 mg $Cr_2O_7^{2-}$ and 139–187 mg CrO_4^{2-} per g of MOF (Tables S2 and S3†). The ReO_4^- sorption isotherms of **PROP-** and **SBUT-MOFs** also show the two-step profile fitted with Langmuir (first step) and Langmuir–Freundlich model (second step), whereas **ET-MOF** displays a one-step isotherm profile fitted only with Freundlich model. The maximum sorption capacities were found between 640 and 960 mg ReO_4^- per g (Fig. S3–S5; Table S4†).

pH-dependent sorption studies. The effect of pH on the Cr (VI) and ReO_4^- removal by alkyl-amino functionalized MOFs was investigated using contaminated solutions in a wide pH range from ∼1 to 10 (±0.02). According to the results depicted in Fig. 4 & S6–S8,† the MOFs can sorb Cr(VI) from solutions with varied pH values, ranging from highly acidic to alkaline conditions. Specifically, the removal percentages from pH 2 to 7 were calculated to be >99% for **PROP-**, **SBUT-**, and **BUT-MOF**, whereas the removal percentage for **ET-MOF** at the same conditions was found to be 96%. Interestingly, these MOFs seem

to be very promising sorbents in acidic solutions of pH ∼ 1 where the removal percentages were calculated to be as high as 89%, 95%, 98%, and 97% for **ET-**, **PROP-**, **SBUT-**, and **BUT-MOF**, respectively, while retain their removal efficiency at pH ∼ 10 where the corresponding percentages are as high as 74%, 78%, 86% and 85% respectively.

As seen from Fig. S9† optimal uptake of ReO_4^- occurred at pH from 3 to 8 with removal percentages at the range of 86–92%. At higher pH values, a small decrease in removal efficiency by **BUT-MOF** was observed at pH ∼ 9 (removal percentage 74%), while decreases sharply at pH ∼ 10 (18%). Likewise, at lower pH values a slight loss of removal performance occurs at pH ∼ 2 with removal percentage of 66% which is further reduced as low as 30% at pH ∼ 1.

Selectivity studies. Another principal factor that affects the efficiency of a sorbent to capture toxic species from wastewater is the coexistence of common anions such as Cl^-, NO_3^- and SO_4^{2-}. We have thus investigated the efficiency of **BUT-MOF** and other analogues to remove selectively Cr(VI) and ReO_4^- in the presence of high excess of the aforementioned anions. The Cr(VI) selectivity study performed with solutions containing either $Cr_2O_7^{2-}$ or CrO_4^{2-} anions, revealed similarities regarding the removal percentages of Cr(VI) (Fig. 5).

Interestingly, **BUT-MOF** retains its sorptive ability in the presence of 100-fold excess of Cl^- or NO_3^- (removal percentages >90% and >85%, respectively), while the MOF displays only a slight loss in solutions containing 1000-fold excess of these anions (removal percentages >80%). Interestingly, in solutions containing 100-fold excess of SO_4^{2-}, which is a strong competitor for Cr(VI) species,[22] Cr(VI) removal percentages are retained relatively high (72 and 75% for $Cr_2O_7^{2-}$ and CrO_4^{2-} respectively). Even when 1000-fold excess of SO_4^{2-} was used, the Cr(VI) sorption efficiencies were appreciable (47% and 44% for $Cr_2O_7^{2-}$ and CrO_4^{2-}, respectively). In addition, we performed antagonistic experiments with ReO_4^- and the selected anions (Fig. S10†). The removal percentages for ReO_4^- in presence of high concentrations of competitive species were not as high as in the case of Cr(VI). Nevertheless, **BUT-MOF** was still able to remove at least a third of the initial ReO_4^- content (initial Re concentration = 50 ppm) in the presence of

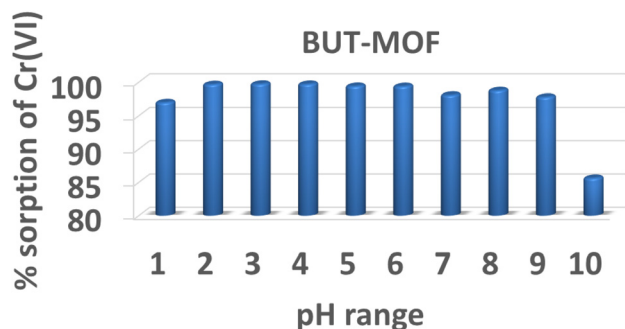**Fig. 4** Percentage (%) sorption of Cr(VI) (0.1 mM) by **BUT-MOF** in the pH range of 1–10.

Fig. 5 $Cr_2O_7^{2-}$ (0.1 mM) and CrO_4^{2-} (0.1 mM) sorption data for **BUT-MOF** in the presence of various competitive anions.

100-fold excess of the competitive anions. As a last step at this study, we performed sorption experiments with bottled water solutions intentionally contaminated with Cr(VI) species or ReO_4^- (Fig. 5 & S10–S12†). These samples contained a variety of competitive anions including Cl^-, NO_3^-, SO_4^{2-} and HCO_3^- (and several cations) in large excess (up to 2.4×10^3-fold) in relation to the oxoanionic species (Table S6†). Similar to the sorption studies in the presence of competitive anions, **BUT-MOF** was more efficient to remove Cr(VI) (80–83% removal) from bottled water samples than ReO_4^- (36% removal). The selectivity of the other MOF analogues for Cr(VI) and ReO_4^- was found similar to that of **BUT-MOF** (Fig. S10–S12†). Presumably, the bivalent Cr(VI) species are expected to interact more strongly than the monoanionic ReO_4^- with the positively-charged surface of **BUT-MOF** (zeta potential = +24.2 ± 5.0 mV),[19] thus leading to the observed higher selectivity of **BUT-MOF** for the Cr(VI) oxoanions. As revealed by the sorption isotherm studies discussed above, relatively low initial concentrations of anions, as those used for the selectivity tests (0.1–0.2 mM) favor mainly surface binding of the oxoanions to MOF particles and under such conditions the driving force for sorption is electrostatic interactions.

Regeneration–reusability studies. As reported in previous publications from our group,[19,22] the regeneration of Zr^{4+} MOFs after anion sorption can be easily achieved via their treatment with a highly acidic solution (4 M HCl). The regeneration of **BUT-MOF** via acidic treatment (ESI†) was verified via IR data, indicating the elimination of the characteristic IR absorption of the inserted anions (Fig. 6). XPS and EDS data, discussed below, also revealed the complete desorption of oxoanions from anion-loaded **BUT-MOF** after the acid treatment.

The regenerated MOF was then reloaded with $Cr_2O_7^{2-}$, CrO_4^{2-} or ReO_4^- anions. IR data (Fig. 6) confirm the sorption of the anions by the MOF, which demonstrates the reusability of **BUT-MOF** as sorbent for oxoanions. The ability of **BUT-MOF** to be regenerated and reused is further proved by the column sorption experiments, discussed in detail below.

Column sorption studies with industrial wastewater samples. In previous works of our group,[22–24] several MOFs in the form of composites with alginic acid mixed with silica sand have been utilized as stationary phase in columns. The content of MOF in the stationary phases of these columns was low (~1% w/w), with the major component being the silica sand. Increasing the content of MOF above 1–2% w/w resulted in slow flow rates and column clogging. It will be important to raise the quantity of MOFs in columns as this would result in enhanced sorption capacities. As a mean to achieve the above, we decided to prepare mm-sized **BUT-MOF/calcium alginate (CA)** beads with a MOF content of ~88% (Fig. S13†) and these beads were then used as stationary phase in a column. Initially, the column was tested for treatment of a Cr(VI) solution of relatively high concentration (19 ppm). The light yellow solution after passing through the column was decolorised and UV-Vis analysis indicated ~98% removal of Cr(VI) (Fig. 7).

Then, the column, operated in up-flow mode (flow rate 2.5 mL min^{-1}) (Fig. S14†), was utilized for the treatment of
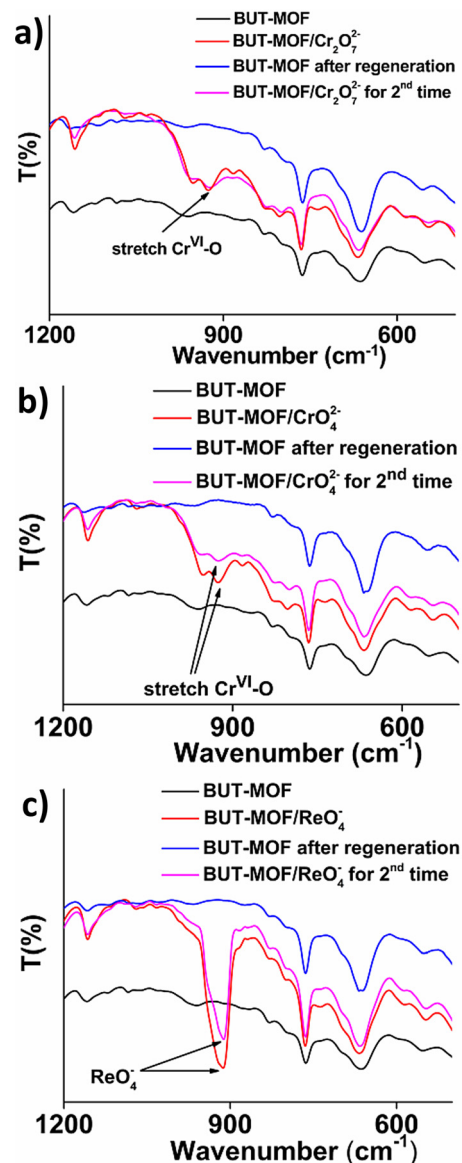
Fig. 6 The IR spectra of the of the ion-loaded **BUT-MOF** (red lines), regenerated **BUT-MOF** (blue lines) and reloaded (purple lines) with (a) $Cr_2O_7^{2-}$, (b) CrO_4^{2-} and (c) ReO_4^-. The arrows point to characteristic ion IR peaks found in the ion-loaded materials. The Cr^{VI}–O stretching IR peak for (a) **BUT-MOF/$Cr_2O_7^{2-}$** and (b) **BUT-MOF/CrO_4^{2-}** was found at 923 cm^{-1}. The ReO_4^- stretching IR peak for (c) **BUT-MOF/ReO_4^-** was found at 916 cm^{-1}.

industrial (chrome-plating) wastewater, containing 330 ppb of Cr(VI). Samples of 400 ml were passed twice through the column, in order to achieve concentrations of the effluents less than 50 ppb (EU-defined upper limit of Cr(VI) in drinking water).[25] For practical applications, two or more columns filled with **BUT-MOF/CA** beads should be utilized for the decontamination of large amounts of wastewater. This is a common practice in wastewater treatment applications, where multicolumn technology is applied to enhance the ion removal efficiencies.[26] In the first run 5.2 L of Cr(VI) solution were passed

Fig. 7 (a) Cr(ʋɪ) industrial waste sorption by the column filled with **BUT-MOF/calcium alginate** beads (initial Cr(ʋɪ) concentration = 19 ppm, pH = 3, 480 mg of sorbent) and (b) UV-Vis spectra of the Cr(ʋɪ) industrial waste solution before and after treatment.

through the column, till reaching a concentration above the acceptable limit of 50 ppb in drinking water (Fig. 8).

However, even after passing such high quantity of wastewater sample, the concentration of Cr(ʋɪ) was well below the acceptable limit of 100 ppb defined by U.S.-EPA.[27] **BUT-MOF/CA** can be easily regenerated by washing the column with 1 M HCl solution. After the regeneration process, a decrease in removal efficiency was observed as a concentration >50 ppb was found when 2 L solution passed through the column. The removal efficiency was further reduced in the next cycles (Fig. 8). Nevertheless, the performance of the **BUT-MOF/CA** column is considered very efficient, since a relatively large amount (∼9 L) of industrial wastewater sample can be purified (*i.e.* contain Cr(ʋɪ) in concentration less than 50 ppb) with only 4 runs of the column. These data are very encouraging for **BUT-MOF** which seems to be a promising sorbent for applications under real-world conditions.

Comparison of BUT-MOF and analogues with other oxoanion MOF sorbents. Till date several MOFs have been tested
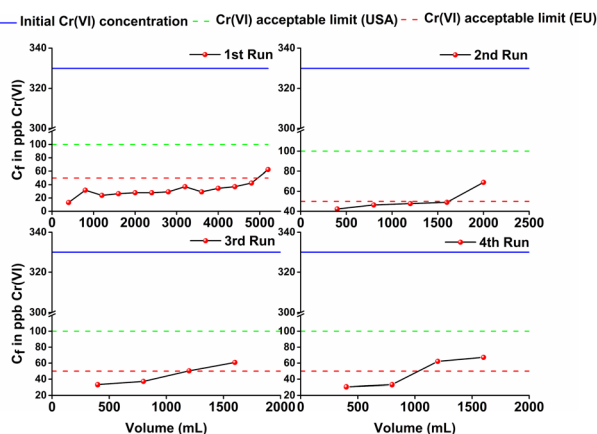
for the removal of Cr(ʋɪ) from aqueous media. In Tables S7 and S8† are provided the most important Cr(ʋɪ) sorption characteristics of **BUT-MOF** and analogues compared with those of other reported MOF-based sorbents. The alkyl-amino functionalized Zr^{4+} MOFs exhibit some of the highest $Cr_2O_7^{2-}$ sorption capacities in combination with rapid sorption kinetics. Among the reported MOFs, only two of them, namely Fe–GA (D) and UTSA-74@FeSO₄, display higher values than **BUT-MOF**.[28,29] However, Fe–gallic acid MOF is not reusable, while for UTSA-74@FeSO₄ MOF regeneration or reusability study is not available. No column sorption data are also presented for the Fe–GA (D) and UTSA-74@FeSO₄ materials and thus, the potential of these sorbents for real applications, usually involving sorption under dynamic conditions, is unknown. In contrary, **BUT-MOF** and analogues combine high maximum sorption capacities, rapid kinetics (equilibrium time ∼ 3 min), efficient performance in the presence of various coexisting anions and reusability. In addition, **BUT-MOF** in the form of **BUT-MOF/CA** beads was successfully utilized in a column for decontamination of large amounts of industrial wastewater samples indicating an attractive sorbent for real world applications. In regards of CrO_4^{2-} removal, the alkyl-amino functionalized MOFs show two to three times higher maximum sorption capacities than most of MOF-based sorbents, with exception of two MOFs reported by our group (MOR-2 and Al-MOF-1) and HPU-13@Fe₃O₄.[22,30,31] In Table S9,† the comparison of sorption characteristics of **ET-**, **PROP-**, **SBUT-** and **BUT-**MOFs with other MOF-based ReO_4^- sorbents indicate that these MOFs are competitive sorbents in terms of maximum sorption capacities, sorption kinetics and regeneration/reusability. Importantly, **BUT-MOF**, along with **MOR-2** reported by our group,[32] is an efficient sorbent even under highly acidic conditions and promising for the decontamination of acidic nuclear waste.

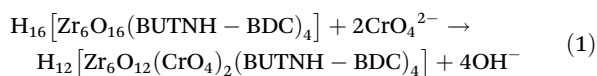### Solid state characterization of the ion-loaded MOFs-mechanism of sorption

The successful binding of the anions on **BUT-MOF** was confirmed *via* several characterization techniques including IR, EDS and XPS data. IR spectra include characteristic peaks at 923 and 916 cm^{-1} attributed to Cr(ʋɪ) and Re(ʋɪɪ) oxoanions respectively (Fig. 6). EDS and XPS confirmed the presence of Cr and Re in the Cr(ʋɪ) and Re(ʋɪɪ)-loaded MOFs (Fig. S15–S17 and Fig. S18–S20†). However, the loaded materials contained no Cl, in contrast to the initial **BUT-MOF** sample (Fig. S15–S21†). Thus, besides the intra-framework binding of the oxoanionic species discussed below, the sorption process also involves exchange of extra-framework Cl^- anions by Cr(ʋɪ) or Re(ʋɪɪ) oxoanions. Furthermore, EDS and XPS data revealed (a) no Re and Cr and (b) presence of Cl for MOF samples after regeneration (Fig. S22–S25†). In addition, high resolution Re 4f and Cr 2p core-level photoelectron spectra for the loaded materials showed binding energies consistent with Re(ʋɪɪ) and Cr(ʋɪ) oxidation states respectively (Fig. S26†).

BET surface area measurements revealed that the surface area of **BUT-MOF** is dramatically decreased after the sorption

Fig. 8 Column sorption data with chrome-plating wastewater sample (flow rate 2.5 mL min⁻¹) containing 330 ppb of Cr(ʋɪ). V_{eff} and C_{eff} are the volume (mL) and Cr(ʋɪ) concentration (ppb) of the solution passed through the column (*i.e.* effluent), respectively.
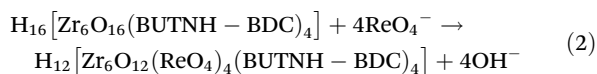
process. This confirms the findings from the isotherm study, that sorption of the anions occurs not only on the surface, *via* exchange of Cl^- and electrostatic interactions of the inserted oxoanions with the positively charged surface of the MOF (see above), but also in the interior of the structure. Specifically, the BET surface area of the pristine **BUT-MOF** was reduced from 609 $m^2 g^{-1}$ to 139, 197, and 370 $m^2 g^{-1}$ after the sorption of $Cr_2O_7^{2-}$, CrO_4^{2-} and ReO_4^-, respectively (Fig. S27†). We should also note that the pore sizes of **BUT-MOF** (5.5–8.5 Å)[19] are large enough to allow diffusion of Cr(VI) and Re(VII) species into the MOF's structure, considering that the radii of hydrated Cr(VI) and Re(VII) oxoanions are 2.4–3.2 Å.[33]

As reported in our previous publication,[19] the terminal OH^-/H_2O ligands in the Zr_6 units of **BUT-MOF** can be replaced by oxoanionic species. Thus, the intra-framework sorption of CrO_4^{2-} by **BUT-MOF** may be described with following equation
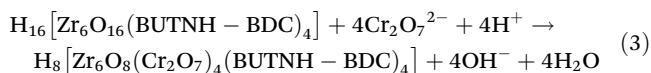
$$H_{16}\left[Zr_6O_{16}(BUTNH-BDC)_4\right] + 2CrO_4^{2-} \rightarrow$$
$$H_{12}\left[Zr_6O_{12}(CrO_4)_2(BUTNH-BDC)_4\right] + 4OH^- \quad (1)$$

According to eqn (1), four terminal OH^- ligands are replaced by 2 CrO_4^{2-} anions. This is in good agreement with the intra-framework CrO_4^{2-} sorption capacity of **BUT-MOF** corresponding to the insertion of ~1.8 moles of CrO_4^{2-} per formula unit of the MOF (see above).

Similarly, the intra-framework capture of ReO_4^- can be described as follows:

$$H_{16}\left[Zr_6O_{16}(BUTNH-BDC)_4\right] + 4ReO_4^- \rightarrow$$
$$H_{12}\left[Zr_6O_{12}(ReO_4)_4(BUTNH-BDC)_4\right] + 4OH^- \quad (2)$$

The replacement of 4 OH^- by 4 ReO_4^- is in good accordance with the sorption results indicating capture of ~4.8 mol of ReO_4^- per formula unit of **BUT-MOF**.

The intra-framework capture of dichromate anions is likely to be described with the following equation:

$$H_{16}\left[Zr_6O_{16}(BUTNH-BDC)_4\right] + 4Cr_2O_7^{2-} + 4H^+ \rightarrow$$
$$H_8\left[Zr_6O_8(Cr_2O_7)_4(BUTNH-BDC)_4\right] + 4OH^- + 4H_2O \quad (3)$$

According to eqn (3), four dichromate anions replace 4 OH^- and 4 H_2O from the Zr_6 building unit and the excess of negative charge due to the insertion of 4 $Cr_2O_7^{2-}$ is compensated by H^+ ions provided by the acidic solution (dichromate sorption proceeds at pH ~ 3). This is in relatively good agreement with the observed intra-framework sorption capacity indicating insertion of 3.45 moles of dichromate per Zr_6 cluster of **BUT-MOF**. The relatively small deviations of the experimental intra-framework sorption capacities from the ideal values are within the errors (10–15%) in the determination of the sorption capacities from the isotherm data.

PXRD patterns, unit cell indexing and Le Bail (structureless) refinement indicate that the structure of the MOF is retained after the sorption of oxoanions (Fig. 9 & S28–S30†). The high crystallinity of the ion-loaded **BUT-MOF** allowed us to solve and refine the structures of these materials *via* PXRD methods. Thus, we built structural models involving 2 CrO_4^{2-},

Fig. 9 Rietveld plots of (a) BUT-MOF/$Cr_2O_7^{2-}$, (b) BUT-MOF/CrO_4^{2-} and (c) BUT-MOF/ReO_4^-. Blue crosses: experimental points; red line: calculated pattern; violet line: difference pattern (exp. – calc.); green bars: Bragg positions. Inset: Magnification of the 2θ region 30–60°.

4 ReO_4^- and 4 $Cr_2O_7^{2-}$ per formula unit of **BUT-MOF**, with the anions initially placed in random positions in the pores. After optimization (simulating annealing) of the initial structural models, chromate and dichromate anions were found to be connected to Zr_6 clusters as bridging ligands, whereas ReO_4^- anions were found to ligate to Zr^{4+} metal ions in a monodentate coordination mode (Fig. 10 & S31–S33†). These coordination modes for Cr(VI) and Re(VIII)-oxoanions are in agreement with those reported for MOR-2, another example of a Zr^{4+}-terephthalate MOF with 8-connected structure.[22,32] Rietveld refinements were satisfactory indicating the accuracy of the proposed structural models (Fig. 9 and ESI†).

Photophysical properties and luminescence sensing

Solid **BUT-MOF** shows a strong cyan fluorescence under UV light irradiation (Fig. S34†). In agreement to our previous studies on a related functionalized Zr^{4+} MOF,[22] an aqueous suspension of **BUT-MOF** at pH = 3 (0.1 mg mL^{-1}) displays a broad fluorescence profile with maximum at *ca.* 490 nm upon excitation at 400 nm. The fluorescence is attributed to the radiative deactivation of the lowest ligand-based singlet excited state, which bears significant charge transfer character since it involves a shift of electron density from the amino group to the aromatic core.[22]

A fluorescence titration where aliquots of a 10^{-4} M aqueous K_2CrO_7 solution were added to a suspension of acid activated **BUT-MOF** leads to strong emission quenching reaching 95% at the end of the titration (Fig. 11a). The calibration curve shows good linearity in the concentration range 0–300 ppb and a linear fit affords limit of detection (LOD) and quantification
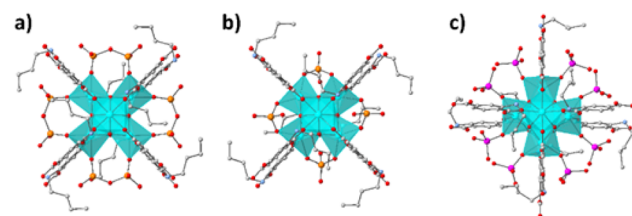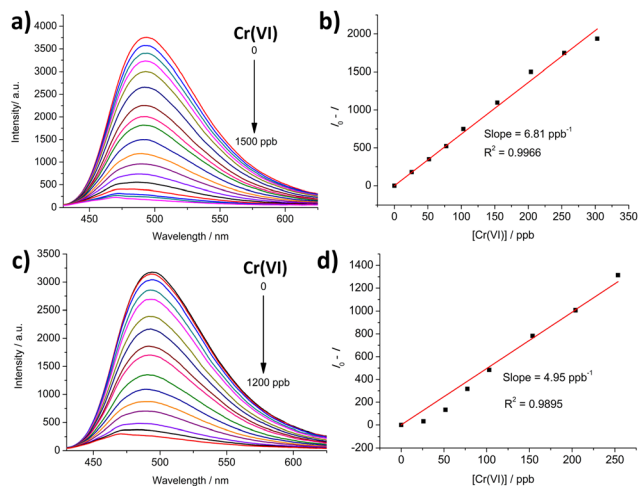

Fig. 10 The coordination mode of (a) $Cr_2O_7^{2-}$, (b) CrO_4^{2-} and (c) ReO_4^- (Cr atoms shown as orange balls; Re atoms shown as purple balls) in the structures of BUT-MOF/$Cr_2O_7^{2-}$, BUT-MOF/CrO_4^{2-} and BUT-MOF/ReO_4^-, respectively, as determined *via* Rietveld refinement (details are discussed in ESI†). H atoms were omitted for clarity.

Fig. 11 (a) Fluorescence titration (λ_{exc} = 400 nm) of acid activated **BUT-MOF** in suspension (0.1 mg mL^{-1}) in distilled water upon the addition of aliquots of a 10^{-4} M solution of $K_2Cr_2O_7$ at pH = 3, (b) calibration curve for the titration in distilled water (black circles correspond to experimental results and the red line corresponds to a linear fit), (c) fluorescence titration (λ_{exc} = 400 nm) of acid activated **BUT-MOF** in suspension (0.1 mg mL^{-1}) in bottled water upon the addition of aliquots of a 10^{-4} M solution of $K_2Cr_2O_7$ at pH = 3 and (d) calibration curve for the titration in bottled water (black circles corresponds to experimental results and the red line corresponds to a linear fit).

(LOQ) values of 9.0 and 30 ppb (Fig. 11b), respectively. Both values are well below the acceptable levels of Cr(VI) in water according to EU (50 ppb) and U.S.-EPA (100 ppb) guidelines.[25,27,34] A Stern–Volmer analysis of the initial linear part of the titration curve yields a Stern–Volmer constant of 3.2 × 10^5 M^{-1} (Fig. S35†). At higher concentrations the Stern–Volmer plot shows an upwards curvature and fits better to a second-degree polynomial. This behavior is consistent with the presence of more than one quenching mechanisms possibly involving collisional (dynamic) quenching in combination with quenching through complex formation (static quenching).[35] As shown in Table S10,† the sensing performance of **BUT-MOF** is comparable to those of the best performing MOF materials found in the recent literature.

Control experiments with 100-fold larger concentrations (10^{-2} M) of NO_3^-, Cl^- and SO_4^{2-} anions show that the material displays only minimal changes in emission intensity (Fig. S36–S38†). Thus, these ions do not induce an emission quenching effect. In agreement with the batch sorption studies (*vide supra*), the presence of a 100-fold excess of Cl^- and NO_3^- only moderately raised the LOD and LOQ values to *ca.* 15 and 50 ppb, respectively (Fig. S39 and S40†). However, when a titration experiment is carried out in the presence of 10-fold excess (10^{-3} M) of SO_4^{2-} anions, as shown in Fig. S41a,† the material displays saturation behaviour much earlier in the titration showing a final quenching percentage of *ca.* 50%. However, interestingly, at the initial stages of the titration the material displays comparable quenching behaviour as that observed in the experiments which are carried out in the absence of SO_4^{2-} anions, as shown by the calibration curve gradient (Fig. S41b†)

corresponding to LOD and LOQ values of 15 and 51 ppb, respectively. This observation may be interpreted by noting that SO_4^{2-} anions are effective competitors to Cr(VI) species (*vide supra*) albeit without inducing appreciable quenching effects to **BUT-MOF** (Fig. S38†). Therefore, the initial quenching shown by **BUT-MOF** is due to its interaction with Cr(VI) species but as the material is exposed to increasing amounts of SO_4^{2-}, the latter block the binding sites, thus preventing further interaction with Cr(VI) anions. In addition, titrations where distilled water is replaced with bottled water containing Cl^- (7.53 ppm), SO_4^{2-} (12.7 ppm) and NO_3^- (8.94 ppm), show a final quenching percentage of 92% and LOD and LOQ values of 12 and 40 ppb (Fig. 11c and d). The values are not much higher than those observed in the absence of competitive species and still lower than the acceptable levels of Cr(VI) in drinking water.

As in our previous work on the related **MOR-2** material,[22] we attribute the quenching behaviour of **BUT-MOF** to energy and/or electron transfer from the photoexcited ligand towards the material's Zr(IV)$_6$ units where Cr(VI) species are attached (*vide supra*).[36]

Conclusions

In summary, this work emphasizes the capability of Zr^{4+} MOFs with low net-connectivity and easily replaceable terminal OH$^-$/H$_2$O ligands to be utilized as efficient sorbents towards toxic and radionuclide-related oxoanions as well as their promising luminescent sensing properties towards Cr(VI). Importantly, **BUT-MOF** and analogues seem to be the most promising sorbents for dichromate anions among reported MOF-based materials, as they combine exceptional maximum sorption capacities (up to 505 mg g^{-1}), quite fast equilibrium sorption times (3 min), limited interference from competitive anions and reusability. Towards real applications, **BUT-MOF**/calcium alginate beads were successfully utilized in a column showing capability for decontamination of relatively large amounts of industrial waste samples. The alkyl-amino functionalized MOFs were also found quite efficient for sorption of CrO_4^{2-} and ReO_4^- oxoanions from aqueous media, thus indicating these MOFs as truly multifunctional anion sorbents. Last but not least, the detailed photophysical investigations revealed that **BUT-MOF** constitutes also a powerful luminescent sensor capable of detecting Cr(VI) in concentrations well-below the acceptable limit in drinking water, even in the presence of several competitive species in large excess.

Author contributions

A. D. Pournara: Investigation, formal analysis, writing – original draft, D. A. Evangelou; Investigation, formal analysis, writing – original draft, C. Roukounaki: Investigation, formal analysis, E. K. Andreou: Investigation, formal analysis, G. S. Armatas: Investigation, formal analysis, writing – review

and editing, T. G. Lazarides: Investigation, formal analysis, writing – review and editing, Manolis J. Manos: Conceptualization, investigation, writing – review and editing, funding acquisition, project administration, supervision.

Conflicts of interest

There are no conflicts to declare.

Acknowledgements

References

1 L. Keith and W. Telliard, *Environ. Sci. Technol.*, 1979, **13**, 416–423.

2 N. Graham, *Urban Water*, 1999, **1**, 183.

3 P. A. Terry, *Chemosphere*, 2004, **57**, 541–546.

4 B. M. Weckhuysen, I. E. Wachs and R. A. Schoonheydt, *Chem. Rev.*, 1996, **96**, 3327–3349.

5 D. Banerjee, D. Kim, M. J. Schweiger, A. A. Kruger and P. K. Thallapally, *Chem. Soc. Rev.*, 2016, **45**, 2724–27396.

6 M. A. Shannon, P. W. Bohn, M. Elimelech, J. G. Georgiadis, B. J. Marĩas and A. M. Mayes, *Nature*, 2008, **452**, 301–310.

7 B. Hu, Y. Ai, J. Jin, T. Hayat, A. Alsaedi, L. Zhuang and X. Wang, *Biochar*, 2020, **2**, 47–64.

8 Y. Choi, M. S. Koo, A. D. Bokare, D. H. Kim, D. W. Bahnemann and W. Choi, *Environ. Sci. Technol.*, 2017, **51**, 3973–3981.

9 G. Chen, J. Feng, W. Wang, Y. Yin and H. Liu, *Water Res.*, 2017, **108**, 383–390.

10 S. Mishra, A. K. Singh and J. K. Singh, *J. Membr. Sci.*, 2020, **593**, 117422.

11 M. Eddaoudi, D. B. Moler, H. Li, B. Chen, T. M. Reineke, M. O'Keeffe and O. M. Yaghi, *Acc. Chem. Res.*, 2001, **34**, 319–330.

12 G. Férey, *Chem. Soc. Rev.*, 2008, **37**, 191–214.

13 S. Horike, S. Shimomura and S. Kitagawa, *Nat. Chem.*, 2009, **1**, 695–704.

14 P. Kumar, A. Pournara, K. H. Kim, V. Bansal, S. Rapti and M. J. Manos, *Prog. Mater. Sci.*, 2017, **86**, 25–74.

15 B. Parmar, K. K. Bisht, Y. Rachuri and E. Suresh, *Inorg. Chem. Front.*, 2020, **7**, 1082–1107.

16 B. Parmar, Y. Rachuri, K. K. Bisht, R. Laiya and E. Suresh, *Inorg. Chem.*, 2017, **56**, 2627–2638.

17 Y. Rachuri, B. Parmar, K. K. Bisht and E. Suresh, *Cryst. Growth Des.*, 2017, **17**, 1363–1372.

18 S. A. Diamantis, A. Margariti, A. D. Pournara, G. S. Papaefstathiou, M. J. Manos and T. Lazarides, *Inorg. Chem. Front.*, 2018, **5**, 1493–1511.

19 A. D. Pournara, S. Rapti, A. Valmas, I. Margiolaki, E. Andreou, G. S. Armatas, A. C. Tsipis, J. C. Plakatouras, D. L. Giokas and M. J. Manos, *J. Mater. Chem. A*, 2021, **9**, 3379–3387.

20 J. D. Law, R. S. Herbst and T. A. Todd, *Sep. Sci. Technol.*, 2002, **37**, 1353–1373.

21 Y. Georgiou, S. Rapti, A. Mavrogiorgou, G. Armatas, M. J. Manos, M. Louloudi and Y. Deligiannakis, *Sci. Rep.*, 2020, **10**, 9358.

22 S. Rapti, D. Sarma, S. A. Diamantis, E. Skliri, G. S. Armatas, A. C. Tsipis, Y. S. Hassan, M. Alkordi, C. D. Malliakas, M. G. Kanatzidis, T. Lazarides, J. C. Plakatouras and M. J. Manos, *J. Mater. Chem. A*, 2017, **5**, 14707–14719.

23 S. Rapti, A. Pournara, D. Sarma, I. T. Papadas, G. S. Armatas, A. C. Tsipis, T. Lazarides, M. G. Kanatzidis and M. J. Manos, *Chem. Sci.*, 2016, **7**, 2427–2436.

24 S. Rapti, A. Pournara, D. Sarma, I. T. Papadas, G. S. Armatas, Y. S. Hassan, M. H. Alkordi, M. G. Kanatzidis and M. J. Manos, *Inorg. Chem. Front.*, 2016, **3**, 635–644.

25 European Comission. Council Directive 98/83/EC on the Quality of Water in-tented for Human Consumption, **http://eurlex.europa.eu/legalcontent/EN/TXT/?uriOCELEX: 31998L0083**.

26 A. A. Zagorodni, *Ion Exchange Materials: Properties and Applications*, Elsevier, 2007, p. 297.

27 USA-EPA, Chromium in Drinking Water, **https://water.epa. gov/drink/info/chromium/**.

28 H. Niu, Y. Zheng, S. Wang, S. He and Y. Cai, *J. Mater. Chem. A*, 2017, **5**, 16600–16604.

29 M. B. Luo, Y. Y. Xiong, H. Q. Wu, X. F. Feng, J. Q. Li and F. Luo, *Angew. Chem., Int. Ed.*, 2017, **56**, 16376–16379.

30 D. Evangelou, A. Pournara, C. Tziasiou, E. Andreou, G. S. Armatas and M. J. Manos, *Inorg. Chem.*, 2022, **61**, 2017–2030.

31 H. Li, Q. Li, X. He, N. Zhang, Z. Xu, Y. Wang and Y. Wang, *Cryst. Growth Des.*, 2018, **18**, 6248–6256.

32 S. Rapti, S. A. Diamantis, A. Dafnomili, A. Pournara, E. Skliri, G. S. Armatas, A. C. Tsipis, I. Spanopoulos, C. D. Malliakas, M. G. Kanatzidis, J. C. Plakatouras, F. Noli, T. Lazarides and M. J. Manos, *J. Mater. Chem. A*, 2018, **6**, 20813–20821.

33 Y. Marcus, *J. Chem. Soc., Faraday Trans.*, 1993, **89**, 713–718.

34 C. Peng, H. Meng, S. Song, S. Lu and A. Lopez-Vaidivieso, *Sep. Sci. Technol.*, 2004, **39**, 1501–1517.

35 J. R. Lakowicz, *Principles of Fluorescence Spectroscopy*, Springer science & business media, 2013.

36 D. Sun, Y. Fu, W. Liu, L. Ye, D. Wang, L. Yang, X. Fu and Z. Li, *Chem. – Eur. J.*, 2013, **19**, 14279–14285.